Zbigniew GMYREK

Technical University of Lodz, Institute of Mechatronics and Information Systems

Modelling of the Properties in Soft Magnetic Material After Punching Process

***Abstract**. The paper deals with the problem of determining the width of the damaged material zone, resulting from the punching process. Using the FEM model and the measurement results, the author propose to apply algorithm which enables determination of magnetic material parameters of the damaged zone. It should be stressed that the proposed algorithm uses non-invasive method of measuring.*

Streszczenie.** Artykuł opisuje problem wyznaczania szerokości strefy zniszczonego materiału, będącej wynikiem procesu wykrawania. Wykorzystując model FEM oraz wyniki pomiarów, autor proponuje algorytm postępowania który umożliwia wyznaczenie szerokości a także właściwości materiału zniszczonej strefy. Należy podkreślić, że proponowany algorytm wykorzystuje bezinwazyjną metodę pomiaru.* ***(Modelowanie właściwości miękkiego materiału magnetycznego poddanego procesowi wykrawania)

Keywords: punching process, magnetic material parameters, magnetic material modeling
Słowa kluczowe: proces wykrawania, właściwości materiału magnetycznego, modelowanie materiału magnetycznego

Introduction

The problem of accurately iron loss determining is studied for many years. Despite the existence of many models describing the ferromagnetic magnetization phenomenon, the problem still remains unresolved. One of the reasons for the difference between the results of measurements and calculations is to omit the influence of mechanical treatment process on magnetic material parameters [1]. In particular, the punch process is the cause of the material degradation. In the past many researchers have analyzed the problem. In [2,3] and [4] we find some information about the influence of the cutting operation on the magnetic material loss. In [5] the authors use a toroidal sample and show the influence of annealing onto magnetic properties after punching process. The first results of a study on the width of the damaged zone which shows the change of internal structure is described in [6]. In this work, it was found that the width may be equal to the thickness of the sheet. It was noted further that there is a clear effect of cutting tools (with blunt or sharp edges) to the significant deterioration of magnetic properties of the damaged material [7]. The authors indicate the existence of several regions of the damaged material as a result of cutting. Many authors point out as the cause of the deterioration of magnetic properties, formation of deformation of the material and the presence of additional internal stresses [8-12]. Efforts are being made to measure the width of the damaged area of the material. Used such invasive methods (drilling holes in the material) to determine the width of the damaged zone is described in articles [9] and [13]. In addition to research results, in the available literature, we find also attempts to model the cutting process and determining losses. An example of interesting research results are described in [14-16]. The author analyzes by FEM model, phenomena in toroidal core subjected to a cutting process. The result of research, aided measurements, is to determine the width, specific loss and permeability curves vs. field strength of the damaged zone. The author suggests to apply a non-invasive method of measurement to determine the parameters described above, what has not been described in literature yet.

Experimental investigations

As well known, the Epstein frame is the international standard for all the energetic and magnetic measurements. Available literature describes many studies that use Epstein frames. Among them there are Epstein frames those have been used for the measure of the iron loss increase due to the punching process [17]. The number or length of punched edges has been increased in the magnetic samples and the iron loss increase has been measured. In this case, the iron loss increase depends on the length of the punched edge. A similar approach has been chosen by the author and toroidal cores have been used as magnetic samples. In the present work two cores have been assembled. The first sample was realized overlapping 45 rings having the inner diameter equal to 120 mm and the outer diameter equal to 200 mm. The used non-oriented magnetic material has a thickness of 0,5 mm. After annealing process this magnetic material has specific losses equal to 4,11 W/kg at 1,5 T/50 Hz. The second sample, first annealed, has been realized with the same external dimensions and number of rings. This sample was assembled with five concentric rings (see Figure1) having width of 8 mm. Test samples had two windings: a primary winding powered by the power supply and the secondary winding used for registration of induced voltage.

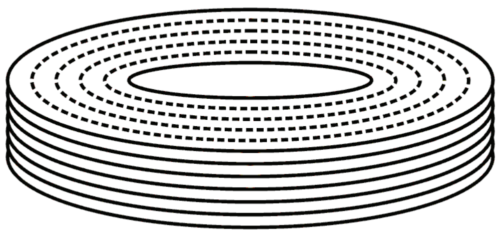

Fig.1. Geometrical characteristic of the core assembled using five concentric rings

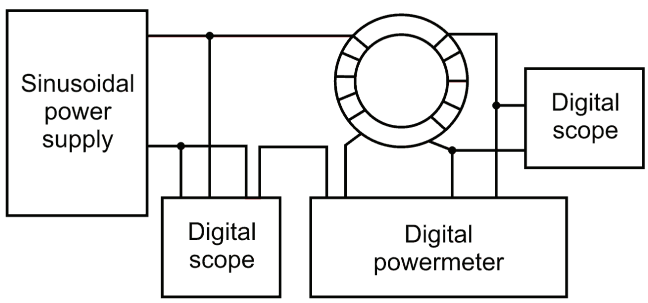

Fig.2 Instrumentation set up for the iron loss measurement.

Measurements were performed in a typical system consisting of a variable sinusoidal voltage supplier and providing digital oscilloscopes, recording waveform of current in the primary winding and waveform of induced voltage in the secondary winding – Fig.2. The variable voltage supply was provided by a sinusoidal power supply (20 KVA, voltage THD < 0,1%). This equipment guarantees that the voltage form factor is close to 1,11, also for high flux density values. The voltage across the shunt resistor (proportional to H) and the induced voltage (proportional to dB/dt) were fed to digital oscilloscopes to measure the iron loss. The B-H curves as well as specific loss curves, measured for both samples are presented in Figures 3 - 4.

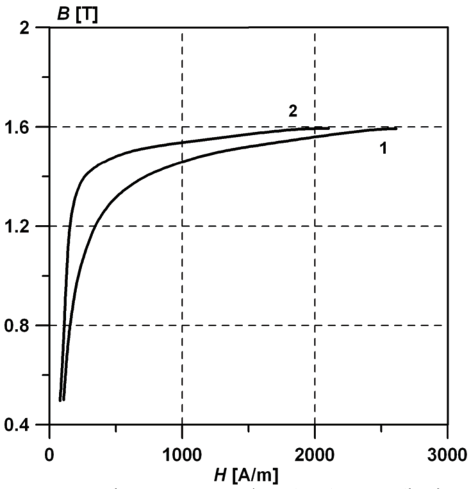

Fig.3 The measured B-H curves. 1 – structure partly damaged due to punching process, 2 – undamaged material structure

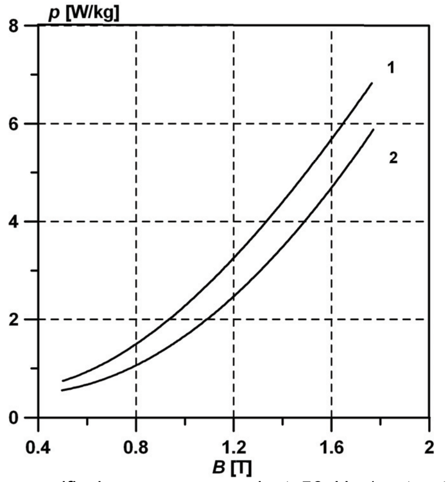

Fig.4 The specific losses measured at 50 Hz.1- structure partly damaged due to punching process, 2- undamaged structure.

FEM approach and calculation results

The FEM models representing the tested toroidal samples were built using the commercial package OPERA 3D. The first model represents a sample made of undamaged material (Fig. 5), while the second one - a sample containing partially damaged material.

Each FEM model contains 350 000 first order elements. In calculations (the magnetostatic problem has been solved) the measured nonlinear B-H characteristic, relating to the undamaged material was used. The results obtained from the electromagnetic calculation were used to find the width of the damaged area of the punched material (what is described later in the paper). To compare the calculated results it was assumed that the maximum magnetic field strength H_{max} is defined by formula

$$H_{\max} = \frac{N\,I_{\max}}{2\,\pi\,r_m} \tag{1}$$

where N is the number of turns, I_{max} is the maximum value of current, r_m is the average radius calculated according to (2), r_e and r_i are the external and internal radiuses respectively.

$$r_m = \frac{r_e - r_i}{\ln\dfrac{r_e}{r_i}} \tag{2}$$

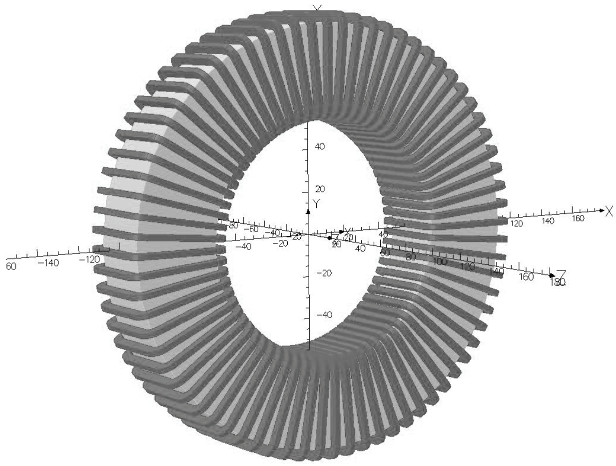

Fig.5 The 3D FEM model of the tested toroidal sample.

First, the FEM model representing the undamaged magnetic material was used. Enforcing the current in the coil (current was defined on the basis of executed measurements) and solving the magnetostatic problem, the flux density distributions were obtained along a specified contour. The contour parameters and its direction, are described below. The two series of calculations were completed: in the first one the currents corresponded to result of measurements carried out for the undamaged material (corresponded to the field strengths H_{nd}), while in the second one the currents corresponded to result of measurements carried out for the partially damaged material (corresponded to the field strengths H_d). The used contour starts at the center of the coordinate system and it is directed along the X axis (direction of X axis is presented in Figure 5). For contour placed in this way, the B_x and B_z components of the flux density vector are close to zero (directions of Z axis and Y axis are visible in Figure 5). This means that for a defined contour only B_y flux density component is important.

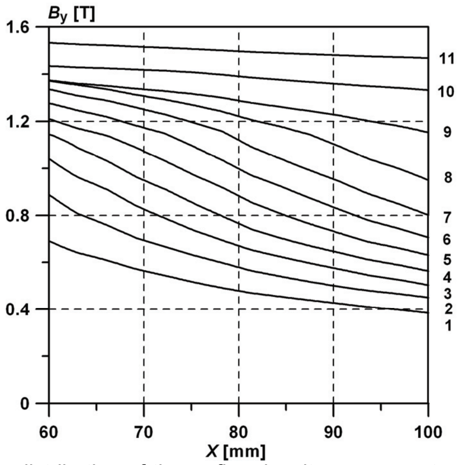

Fig.6 The distribution of the B_y flux density component vs. contour X coordinate. Undamaged material. Numbers from 1 to 11 refer to the corresponding magnetic field strengths H_{nd} shown in Table 1

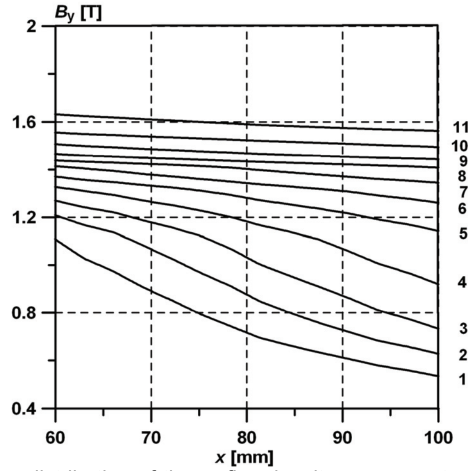

Fig.7 The distribution of the B_y flux density component vs. contour X coordinate. Undamaged material. Numbers from 1 to 11 refer to the corresponding magnetic field strengths H_d shown in Table 1

Since the inner radius equal to 60 mm and outer radius equal to 100 mm, so the distribution of the B_y flux density component was presented in a range from 60 to 100 mm – see Figures 6-7. These distributions were determined for several values of magnetic field strength corresponding to the accepted average values of induction B_{AV} – see Table 1. In partially damaged material to achieve the same average flux density as in undamaged material, it is necessary to enforce a magnetic field strength $H_d > H_{nd}$. As a result, in undamaged material and excitation proportional to H_d there is the greater B_{AVD} flux density. Calculated the average B_{AVD} flux density values are presented in Table 2.

Table 1. The values of the magnetic field strength for the undamaged material (H_{nd}) and for damaged material (H_d), measured for specified B_{AV} flux density .

B_{AV} [T]	0,5	0,6	0,7	0,8	0,9	1,0
H_{ND} [A/m]	79	91	102	111	119	128
H_D [A/m]	106	120	134	154	182	217
B_{AV} [T]	1,1	1,2	1,3	1,4	1,5	
H_{ND} [A/m]	137	154	185	263	583	
H_D [A/m]	271	344	467	706	1222	

Table 2. The B_{AVD} flux density values calculated for magnetic field strength H_d in undamaged material

H_D [A/m]	106	120	134	154	182	217
B_{AVD} [T]	0,75	0,90	1,05	1,20	1,29	1,35
H_D [A/m]	271	344	467	706	1222	
B_{AVD} [T]	1,41	1,45	1,48	1,51	1,55	

Based on the results of experiments described in the available literature, it can be concluded that the damaged material has far worse magnetic parameters in comparison with the undamaged material (especially for the flux density in the range from 0,6 T to 0,8T – for the investigated material). In order to estimate the minimum width of the damaged area, the author suggests making the following assumption: flux density equals 0 in the damaged zones when the measured average flux density B_{AV} is lower than 0,8 T (the excitation field strength is H_d). Knowing the radii of punching (for individual rings), in calculated flux density distributions set for H_d magnetic field strength, the width of the area representing damaged material was increased, to reach an average flux density value below the expected B_{AV} (with specified ε error). To achieve this goal, the second FEM model was used, in which: the width of the damaged zone was changed; in the damaged part of the material the relative magnetic permeability was assumed equal to 0; in the undamaged part of the magnetic material the non-linear B-H curve was assumed; the currents corresponding to the H_d field strength were forced. The applied algorithm changes damaged zone width as long as the calculated error ε is below the specified value. The ε error was determined by following formula

$$\varepsilon = \frac{\sqrt{\left(B_{AV} - \frac{1}{n}\sum_{i=1}^{n} B_i\right)^2}}{B_{AV}} \tag{3}$$

where n is the number of points in a contour, B_i is the calculated flux density at i-th point of the contour (determined for the field strength H_d), B_{AV} is the expected average value of flux density.

On the basis of the calculations performed, it was found that the minimum width of the damaged zone near the cut edge is equal to 1,2 mm (it was assumed that this width is identical for all five rings). The example of the flux density distribution, taking the damaged areas into account, is shown in Figure 8.

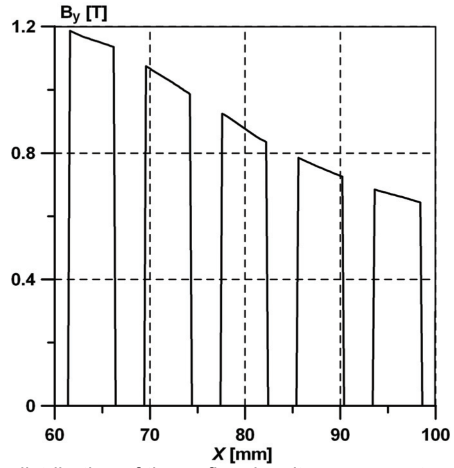

Fig.8 The distribution of the B_y flux density component vs. contour X coordinate. Results determined for the magnetic field strength H_d equal to 120 A/m. The width of the damaged zone equals 1,2 mm. In the damaged zone the flux equals 0.

Another problem is the estimation of the maximum width of the damaged material zone. The maximum width of the damaged zone was determined based on the measurement results carried out for a package made of rings having a width of 40 mm. It was found that the specific loss increase (for this package with respect to specific loss determined for annealed material) is five times smaller than that for a package made up of five concentric rings. This means that the width of the damaged zone near punched edge is less than 4 mm (which is a half the width of one of the five concentric rings). Knowing the range in which the width of the damaged zone exists, the author began to define its width more accurately. In this discussion the author assumes that the magnetic permeability of the material in damaged zone is dependent only on the current value of the magnetic field strength. As we know from the available literature the change of magnetic properties depends on the current value of the tensions inside the material structure. These tensions vary with distance from the punched edge. But it is known that only in not very high tension range the rapid changes in magnetic properties occur. These changes for larger tensions are not violent. In this respect the author assumes that the internal tension distribution is identical across the damaged zone, which authorizes the adoption such assumption: the magnetic permeability is dependent on the magnetic field strength only (of course it is quite different than magnetic permeability for undamaged material for the same magnetic field strength). Since, the damaged zone permeability is a function of the magnetic field strength only. First, the initially estimated magnetic permeability (for specified magnetic field strength) was determined based on knowledge of the Λ magnetic conductivity. In the case of partially damaged magnetic material, there are side by side areas with different Λ magnetic conductivities. Then the resultant magnetic conductivity of the area having cross-section A is equal to the sum of the conductivity of an area having cross-section $A1=h(a-x)$ and the conductivity of an area having cross-section $A2=hx$. Of course, the sum of components $A1$ and $A2$ equals A – see Fig. 9. Thus, it becomes possible to estimate the magnetic permeability of the damaged area as a function of its width x

(4) $$\mu_x = \mu_1 - \frac{(\mu_1 - \mu_{AV})a}{x}$$

where μ_x is the magnetic permeability of damaged material, μ_1 is the magnetic permeability of undamaged material (for the field strength H_d), μ_{AV} is the measured magnetic permeability (for the average flux density B_{AV}), a is the material width (40 mm), x is the unkown total zone width near cut edge.

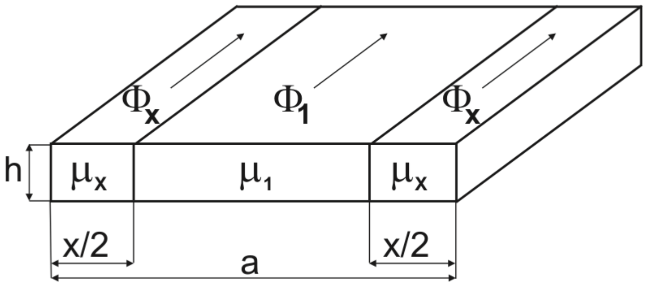

Fig.9 A magnetic material with two marked regions.

Table 3. The estimated relative magnetic permeability μ_{Rx} determined for some total damaged zone widths.

H_d [A/m]	1222					
x [mm]	12	14	16	18	20	22
μ_{Rx} [-]	907	922	934	943	950	956
H_d [A/m]			706			
x [mm]	12	14	16	18	20	22
μ_{Rx} [-]	1294	1354	1398	1433	1461	1484
H_d [A/m]			467			
x [mm]	12	14	16	18	20	22
μ_{Rx} [-]	1508	1655	1765	1851	1919	1975

Next step was performed to more accurately estimate the width of the zone, assuming that all the damaged zones have the same widths. To do this we have to find two equations binding the damaged zone permeability and its width. We can achieve this by writing the following equations:

(5) $$B_{AV}ah = B_x xh + B_{AVD}(a-x)h$$

where h is the height of magnetic core, B_{AV} is the average flux density for partially damaged material, B_x is the flux density for the damaged part of the material, B_{AVD} is the flux density for undamaged material.

(6) $$p_{AV}ahl\rho = cB_x^2 xhl\rho + p_1(a-x)hl\rho$$

where p_{AV} is the measured specific loss for partially damaged material, p_1 is the measured specific loss for undamaged material (determined for calculated flux density B_{AVD}), ρ is the mass density, l is the magnetic circuit length, c is the specific loss constant.

In formula (6) it was adopted that the specific losses in the damaged zone are proportional to the square of the flux density. This relationship was determined on the basis of the loss component measurements, executed for the undamaged and damaged materials, in specified flux density range. For the undamaged material hysteresis losses are proportional to $B^{2.1}$ whereas for damaged material they are proportional to $B^{2.0}$.

The c constant could be eliminated from the above equation by writing a new equation for new work conditions. Determining the induction B_x from equation (5) and inserting it into equation (6), after ordering we obtain

(7) $$p_{AV}a = c\frac{((B_{AV} - B_{AVD})a + B_{AVD}x)^2}{x} + p_1(a-x)$$

Some data used to determine the width of the damaged material zone are given in Table 4. In the calculations the following pairs of data for the B_{AV} flux densities were used (1,5 T, 1,45 T), (1,45 T, 1,4 T) and (1,35 T, 1,3 T). Then the following pair of results for the damaged zone widths were obtained (in mm): 0,17 and 1,62, 0,25 and 2,0, 0,36 and 2,0. As previously demonstrated the minimum zone width is equal to 1,2 mm, so it was necessary to reject the results of calculations that do not meet this criterion. Then, using the remaining results, the mean value was calculated and accepted as the proper width of the damaged zone. The proper value equals 1,87 mm. Please note the dependence of p_1 and p_{AV} specific losses on the B_{AV} flux density, presented in Table 4. For the B_{AV} flux density equals 1,5 T the p_{AV} specific loss is greater than the p_1 specific loss whereas for the flux density equals 1,3 T p_{AV} is smaller than p_1. This trend also occurs for the lower B_{AV} flux density. This confirms the earlier assumption that for the small flux density B_{AV} it can be pre-assumed that the flux density in the damaged area is close to zero. For larger B_{AV} flux density this assumption may not be accepted.

Table 4. The measured and calculated data needed to determine the damaged zone width.

B_{AV} [T]	1,5	1,45	1,4	1,35	1,3
B_{AVD} [T]	1,55	1,53	1,51	1,49	1,48
p_{AV} [W/kg]	5,02	4,68	4,32	4,04	3,72
p_1 [W/kg]	4,46	4,31	4,16	4,01	3,94

After estimating the proper zone width of the damaged material, the magnetization curve of the damaged material was determined. The calculation process started with the magnetic field strength which equals 1222 A/m. Knowing the zone width, the part of the magnetization curve should be found using the calculated average flux density B_{AV} which should reach 1,5 T. The magnetic material is nonlinear and the magnetic field strength on the surface depends on the current radius, so it is necessary to designate the fragment of the magnetization curve, not a single magnetic permeability value. This part of the curve will not change during next calculations. The magnetization curve of the damaged material was approximated by a cubic spline, using initially estimated magnetic permeabilities calculated with help of the known zone width, according to (4). For each B_{AV} a minimum and maximum magnetic field strengths (on the sample surface) are known because they result from the ampere-turns as well as the inner radius and outer radius of the sample. For such a range of magnetic field strength, the magnetization curve was mapped by a third-degree polynomial.

For a pre-set material damage zone width, the proposed algorithm has found the polynomial coefficients so as to achieve the minimum error described by the equation (3). The B_i induction values were calculated with the aid of a FEM model and the currently used polynomial representing a part of magnetization curve for damaged material. Then, the next interval of the magnetic field strength was fixed and for this interval the next third-order polynomial was determined. In this way the magnetization curve of the damaged material has been found – see Figure 10. As a result of calculations carried out, a new flux density distribution was received - see Figure 11. As it is clear from the presented distribution, flux density in the damaged areas is three times smaller than in the adjacent undamaged areas. Flux density step change between damaged and undamaged areas of the material is the result of accepted simplifying assumptions.

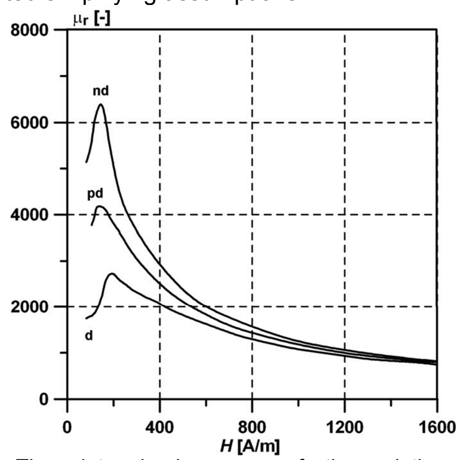

Fig.10 The determined curves of the relative magnetic permeability. d – the calculated curve for damaged material, nd – the measured curve for undamaged material, pd - the measured curve for partially damaged material. The width of the damaged zone equals 1,87 mm.

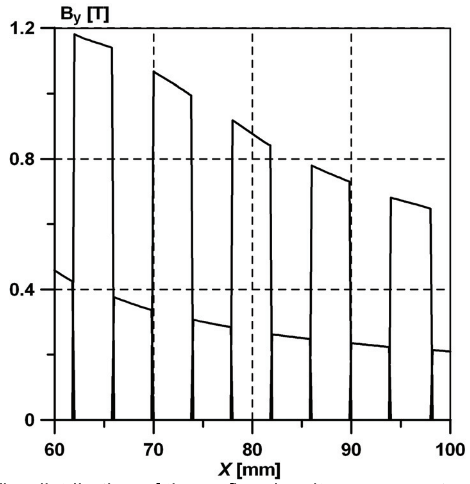

Fig.11 The distribution of the B_y flux density component vs. contour X coordinate. The magnetic field strength H_d - 120 A/m, both magnetization curves included. The width of the damaged zone – 1,87 mm.

After determining the width and the relative permeability curve of the damaged zone, it was possible to determine the specific loss of the damaged material. To accomplish this task it is necessary to obtain knowledge about: specific iron loss dependence on the flux density of the undamaged material; the total losses measured in the sample; the distribution of the flux density in the sample containing partially damaged material. Based on measurements the same specific loss vs. flux density dependence (power of flux density) has been found, both for the undamaged and damaged materials (of course the aspect ratio was different for the damaged and undamaged material). The procedure for determining the specific loss curve of the damaged material is identical to that which was applied when the relative permeability curve was determined. In this case, the procedure minimizes the error determined by the formula

$$\varepsilon = \frac{\sqrt{\left(p_{meas} - \frac{1}{n}\sum_{i=1}^{n} p_{cal\,i}\right)^2}}{p_{meas}} \tag{8}$$

where n is the number of elementary volumes, p_{cali} is the calculated specific loss in i-th elementary volume, p_{meas} is the measured specific loss, both determined for the same specified B_{AV} flux density.

As a result of the calculations executed, the specific loss curve of the damaged material was determined and reported in Figure 12. In fact, it is interesting to observe that the partially damaged material is between the *a* and *c* curves. Using the specific loss curve for the damaged and undamaged materials some examples of specific loss distribution in the sample are presented in Figures 13-14.

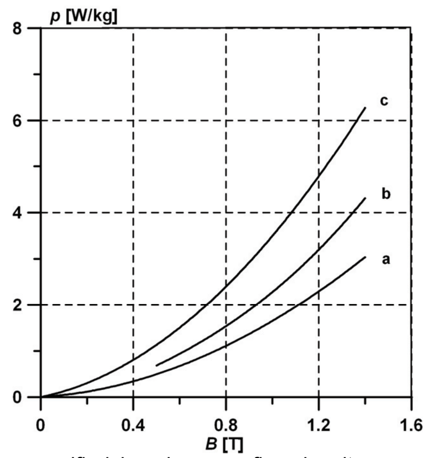

Fig.12 The specified iron loss vs. flux density. a – undamaged material, b– measured for partially damaged material, c– damaged material. The width of the damaged zone equals 1.87 mm.

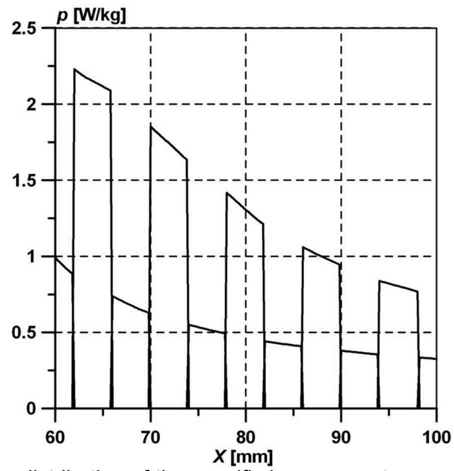

Fig.13 The distribution of the specific loss vs. contour X coordinate. The magnetic field strength H_d equals 120 A/m. The width of the damaged zone equals 1.87 mm.

Comparison of measured and calculated specific loss is presented in Table 5.

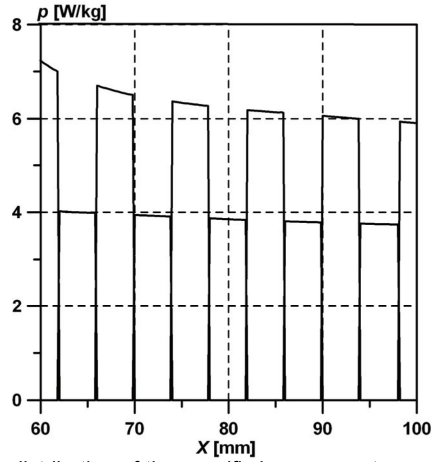

Fig.14 The distribution of the specific loss vs. contour X coordinate. The magnetic field strength H_d equals 1222 A/m. The width of the damaged zone equals 1.87 mm.

Table 5. The comparison of measured and calculated specific loss in tested sample, determined for specified B_{AV} flux density .

B_{AV} [T]	0,5	0,6	0,7	0,8	0,9	1,0	1,1	1,2	1,3	1,4	1,5
p_{ND} [W/kg]	0,5	0,67	0,85	1,07	1,28	1,41	1,53	1,61	1,68	1,79	1,95
p_D [W/kg]	0,19	0,25	0,32	0,47	0,71	0,84	1,20	1,54	2,02	2,56	3,10
p^*_{DCAL} [W/kg[	0,69	0,92	1,17	1,54	1,99	2,25	2,73	3,15	3,70	4,35	5,05
p^*_{DMEAS} [W/kg]	0,69	0,94	1,22	1,53	1,90	2,29	2,72	3,19	3,72	4,32	5,02

where p_{ND} is the calculated average specific loss determined for the non-destructed part of the sample, p_D is the calculated average specific loss determined for the destructed part of the sample, p^*_{DCAL} is the calculated specific loss determined for the sample, p^*_{DMEAS} is the measured specific loss determined for the sample.

Conclusion

The author proposed a method for determination of the damaged zone width. The damaged zone results from the execution of punching process. In the proposed method the 3D FEM model and the results of the measurements were used. The data necessary for calculation is based on simple non-invasive measurements. Then, the author proposes a computational algorithm that uses: fixed width of the damaged zone, the results of the measurements and the adopted model of the magnetic material. The accepted model of magnetic material assumes that the magnetic material properties of the damaged zone, depend only on the magnetic field strength. This means that these properties do not depend on the current distance to the cutting edge. Adequacy of the adopted assumptions has been verified by the adoption of another magnetic material model, defining variability of the magnetic material properties. This will be described in subsequent papers, which are in preparation. The performance of the proposed way of proceedings was verified by the measurement, yielding very good agreement. The complete verification of the proposed approach needs to be supported by additional research carried out on the analyzed samples; for this reason further experimental investigations are ongoing. However, the obtained results correspond very well are in good agreements with the results of other researchers described in the literature.

REFERENCES

[1] Schoppa A., Schneider J., Wuppermann C.-D., Influence of the manufacturing process on the magnetic properties of non-oriented electrical steels, *JMMM*, 215-216, 2000, pp.74-78
[2] Belgrand T., Eple S., Tell us about your punch, we'll tell you about your electrical steel magnetic properties, *Journal de Physique*, vol.8, 1998, pp.611-614
[3] Schoppa A., Louis H., Pude F., Von Rad Ch., Influence of abrasive waterjet cutting on the magnetic properties of non-oriented electrical steels, *JMMM*, 254-255, 2003, pp.370-372
[4] Wilczyński W. Talik S., Szubzda B., Porównanie wpływu wykrawania i cięcia laserem blach elektrotechnicznych na ich własności magnetyczne, *Przegląd Elektrotechniczny*, 2003, No 2, pp. 160-163
[5] Boglietti A., Cavagnino A., Ferraris L., Lazzari M., The annealing influence onto the magnetic and energetic properties in soft magnetic material after punching process, *Conf. Rec. IEEE-IEMDC'2003*, Madison, Wisconsin, USA, IEEE catalog number 03EX679C, ISBN 0-7803-7818-0, pp. 503-508.
[6] Schmidt K. H., Influence of punching on the magnetic properties of electric steel with 1% silicon, JMMM, 1976, pp.136-150
[7] Baudouin P., De Wulf M., Kestens L., Houbaert Y., The effect of the quillotine clearance on the magnetic properties of electrical steels, *JMMM*, 256, 2003, pp.32-40
[8] Rygał R., Moses A. J., Derebasi N., Schneider J., Schoppa A., Influence of cutting stress on magnetic field and flux density distribution in non-oriented electrical steels, *JMMM*, 215-216, 2000, pp.687-689
[9] Dupre L. R., Fiorillo F., Melkebeek J., Rietto A. M., Appino C., Loss versus cutting angle in grain-oriented Fe-Si laminations, *JMMM*, 215-216, 2000, pp.112-114
[10] Schoppa A., Schneider J., Roth J.-O., Influence of the cutting process on the magnetic properties of non-oriented electrical steels, *JMMM*, 215-216, 2000, pp.100-102
[11] Nakata T., Nakano K., Kawahara K., Effect of stress due to cutting on magnetic characteristics of silicon steel, *IEEE Transaction on Magnetics* in Japan 7 (6), 1992, pp.453-457
[12] Pulnikov A., Baudowin P., Melkebeek J., Induced stresses due to the mechanical cutting of non-oriented electrical steels, *JMMM*, 245-255, 2003, pp.355-357
[13] Moses A. J., Derebasi N., Loisos G., Schoppa A., Aspects of the cut-edge stress on the power loss and flux density distribution in electrical steel sheets, *JMMM*, 215-216, 2000, pp.690-692
[14] Crevecoeur G., Sergeant P., Dupre L., Vandenbossche L.,. Van de Welle R, Analysis of the local material degradation near cutting edges of electrical steel sheets, *IEEE Transaction on Magnetics*, 2008, No 44, pp.3173-3176
[15] Crevecoeur G., Dupre L., Vandenbossche L., Van de Welle R., Local identification of magnetic hysteresis properties near cutting edges of electrical steel sheets, *IEEE Transaction on Magnetics*, 2008, No 44, pp.1010-1013
[16] Goes P., DeWulf M., Calculating iron losses taking into account effects of manufacturing processes, *Proc. of COMSOL Conference*, Hannover, 2008
[17] Smith A. C., Edey K., Influence of manufacturing processes on iron losses, *Proc. of the Electrical Machines and Drives,* IEE Conference Publication, 1995, No. 142, pp. 77-81

Author: *dr hab. inż. Zbigniew Gmyrek, Politechnika Łódzka, Instytut Mechatroniki i Systemów Informatycznych, ul. Stefanowskiego 18/22, 90-924 Łódź, Poland, e-mail: zbigniew.gmyrek@p.lodz.pl*